STATE OF OREGON
DEPARTMENT OF GEOLOGY AND MINERAL INDUSTRIES
www.OregonGeology.org
W. Lawrence Givens, Governing Board Chair
Vicki S. McConnell, Director and State Geologist
Andrew V. Pollock, Assistant Director, Geologic Survey and Services
Rachel L. Smith, Project Operations Manager
Ian P. Madin, Chief Scientist

Geologic Map of Part of the Upper Soda and Harter Mountain 7.5' Quadrangles, Oregon

2013

OPEN-FILE REPORT O-13-23

Silicic Volcanism in the Menagerie Wilderness and Adjacent Regions of the Western Cascades in Oregon

by Geoffrey W. Cook, Craig M. White, and James L. Crowley

PLATE 1 (APPENDIX A)

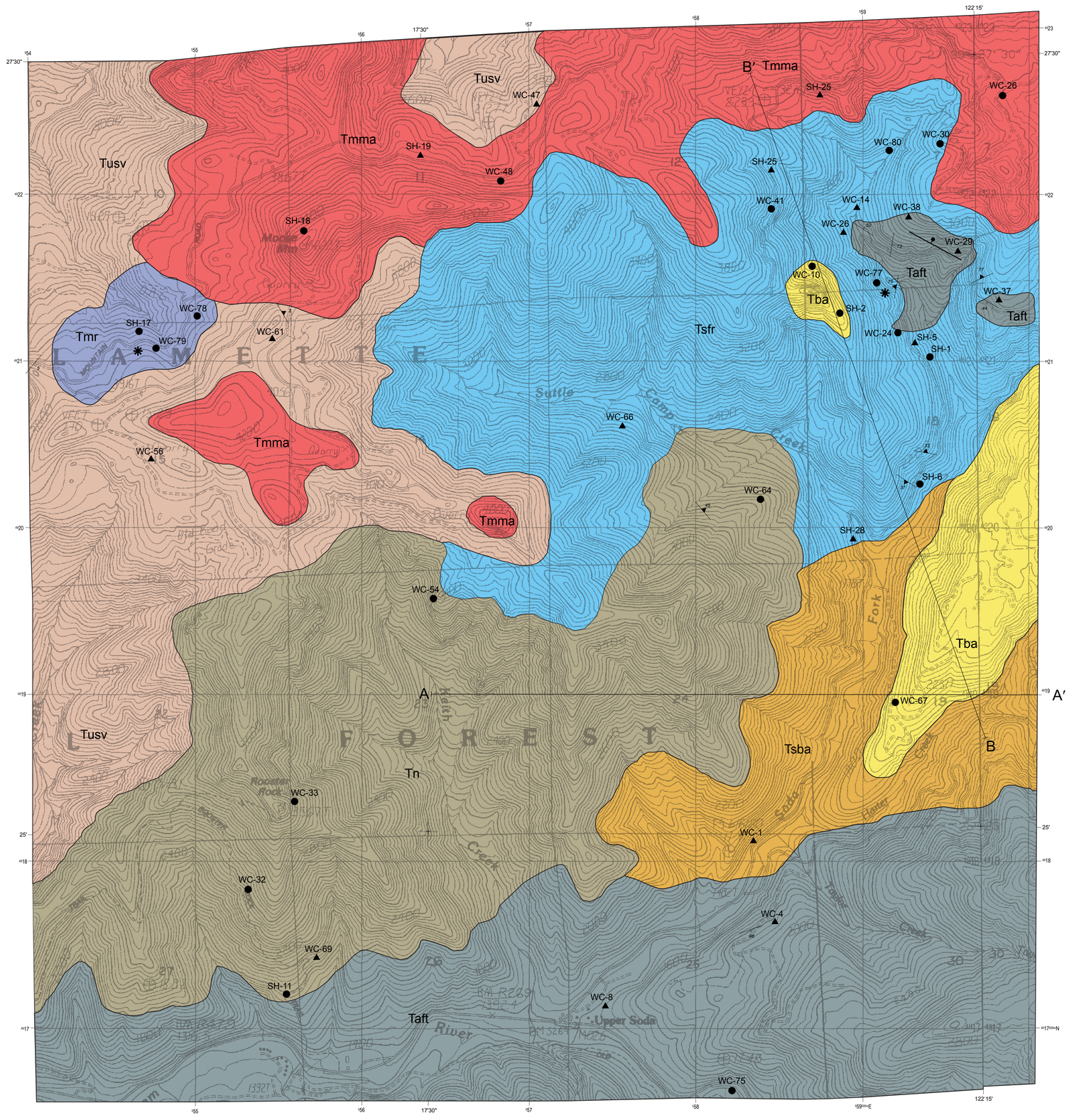

Base map by United States Geological Survey

Control by USGS and NOS/NOAA

Topography compiled from aerial photographs taken 1976 and 1980. Field checked 1982. Map edited 1985. Provisional edition

Projection: Lambert conformal conic projection
Grid: 1000 meter Universal Transverse Mercator, Zone 10
10,000 foot state grid ticks - Oregon, North Zone
UTM grid declination 0° 29' east
1980 magnetic north declination, 19° east
Vertical datum - National geodetic vertical datum of 1929
Horizontal datum - 1927 North American datum

SCALE 1:12,000

NORTH

0.5 0 KILOMETERS 500 1
500 0 METERS 500 1000
0.5 0 0.5
MILES

QUADRANGLE LOCATION

1	2	3
4	5	6
6	7	8

1 Yellowstone Mtn.
2 Quartville
3 Chimney Mtn.
4 Cascadia
5 Upper Soda
6 Harter Mtn.
7 Swamp Mtn.
8 Tidbits Mtn.
9 Carpenter Mtn.

ADJOINING 7.5' QUADRANGLE NAMES

Geology and cartography by Geoffrey W. Cook
Field work conducted in 2001

EXPLANATION OF MAP UNITS

See accompanying pamphlet for detailed descriptions of silicic units.

Pliocene (?)

- **Tba** — Basaltic andesite lava flows, some with well-developed columnar joints. Flows are porphyritic with plagioclase phenocrysts to 2 mm and clinopyroxene phenocrysts to 2.5 mm. Unit is approximately 130 m thick.
- **Tmma** — Two-pyroxene andesite and basaltic andesite lava flows. Flows are generally porphyritic with plagioclase phenocrysts visible to 5 mm and pyroxene to 2.5 mm. The unit is informally referred to as the andesite of Moose Mountain.

Miocene

- **Tmr** — Devitrified porphyritic rhyolite flows; phenocrysts include biotite and hornblende to 1 mm, plagioclase and anorthoclase to 2 mm, and embayed phenocrysts of quartz to 4 mm. Unit is an endogenous dome complex approximately 130 m thick and is informally referred to as the rhyolite of Moose Mountain.
- **Tusv** — Undifferentiated ash flows, air falls, and flow-banded rhyolites. Unit is at least 330 m thick. Unit is poorly exposed, and stratigraphic relationships are unclear.
- **Tsba** — Block and ash flow deposits containing block-sized fragments of unit Tsfr. Unit is approximately 240 m thick. The unit is informally referred to as the block and ash flows of Soda Fork.
- **Tsfr** — Pinkish flow-banded rhyolite. Unit is an exogenous dome approximately 430 m thick with multiple flows and vent complexes. Flows vary in nature from devitrified and spherulitic to vitrophyric along flow boundaries. Phenocrysts present include plagioclase to 5 mm, anorthoclase to 4 mm, resorbed quartz to 2 mm, and pyroxene to 2 mm in the vitrophyre. The lack of hornblende in this unit helps differentiate it from the Rooster Rock complex. The unit is informally referred to as the rhyolite of Soda Fork.
- **Trr** — Light gray, porphyritic rhyolite with hornblende phenocrysts to 1 cm. Unit is an endogenous dome complex approximately 800 m thick. Unit is informally referred to as the rhyolite of Rooster Rock.
- **Taft** — Lithic-rich ash flow tuffs; moderately to strongly welded and interbedded with thin ash fall deposits to 10 cm. May contain localized block and ash flows with lithic fragments to 5 cm. Unit is at least 570 m thick. The unit is informally referred to as the ash flow tuffs of Route 20.

MAP SYMBOLS

- Depositional contact; all contacts inferred
- Normal fault; tick marks on structurally lowest block
- ● Sample location with geochemistry and thin section (see Table 1)
- ▲ Sample location with thin section only
- ✱ Location of inferred volcanic vent
- 44 Strike and dip of bedding
- 77 Flow foliation

Table 1. Whole-rock XRF analyses for samples denoted on map. See accompanying pamphlet for analytical methods.

Sample	SiO_2	TiO_2	Al_2O_3	FeO	MnO	MgO	CaO	Na_2O	K_2O
*SH1	72.90	0.26	14.90	1.57	0.05	0.01	0.82	5.92	3.08
*SH2	54.40	0.96	17.70	6.64	0.11	3.61	7.89	3.35	1.13
*SH6	72.80	0.26	13.70	1.85	0.04	0.31	1.27	4.54	2.97
*SH11	67.70	0.51	15.30	3.83	0.09	1.70	1.46	5.41	1.82
*SH17	74.10	0.19	13.80	1.14	0.01	0.02	1.11	4.58	3.62
**WC77	73.62	0.29	14.45	1.60	0.03	0.17	0.70	5.28	3.57
**WC80	76.58	0.31	12.78	1.73	0.01	0.11	0.54	2.97	4.27
**WC24	71.39	0.25	16.19	1.58	0.06	0.18	0.49	6.97	2.51
**WC30	74.22	0.34	14.10	2.12	0.01	0.12	1.36	4.41	2.86
**WC41	74.67	0.34	13.50	2.03	0.02	0.12	1.10	3.71	3.92
**WC75	51.09	1.20	18.16	8.11	0.14	4.45	8.53	3.65	1.04
**WC78	78.68	0.20	11.99	1.14	0.01	0.24	1.25	3.50	2.71
**WC79	77.87	0.21	12.38	1.09	0.01	0.23	1.26	3.53	2.83
**WC26	58.58	1.05	17.74	6.17	0.13	3.21	6.86	4.27	1.03
**WC10	55.47	1.02	18.76	6.25	0.14	4.56	8.60	3.56	0.92
**WC67	54.40	1.28	17.91	6.45	0.12	5.69	8.70	3.74	1.10
**WC48	62.62	0.94	15.85	4.86	0.08	2.91	4.61	4.12	2.04
**WC54	73.19	0.36	14.46	2.39	0.03	0.56	0.51	3.23	3.89
**WC32	71.80	0.39	14.14	2.53	0.03	0.74	1.60	4.05	2.79
**WC33	72.71	0.38	14.64	2.42	0.03	0.52	0.48	3.17	3.94
**WC64	74.74	0.24	14.08	1.55	0.03	0.17	0.45	4.64	3.26

* XRF analyses performed at XRAL Laboratory, Toronto (C. M. White, unpublished data).
** XRF analyses performed at Washington State University GeoAnalytical Lab (G.W. Cook, 2001, Petrology and geochemistry of Western Cascade silicic volcanics, Menagerie Wilderness, Oregon; M.S. thesis, Boise State University, Boise, ID).

GEOLOGIC CROSS SECTIONS

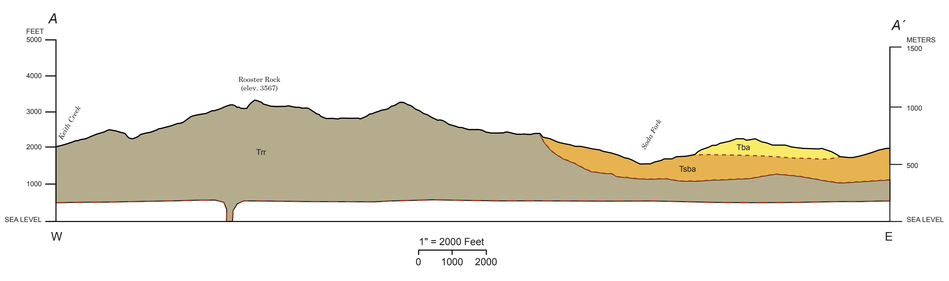

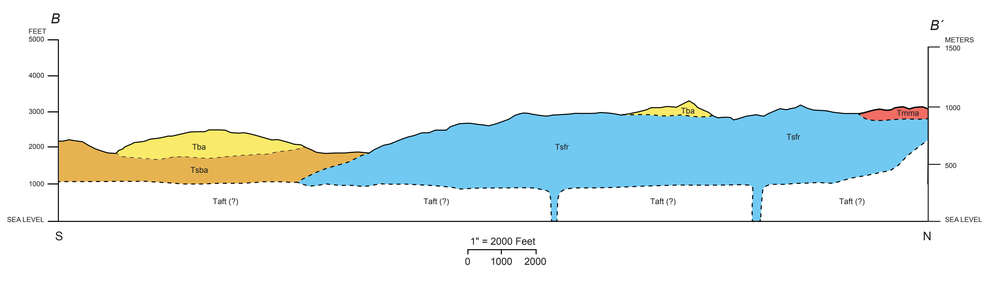

Nature of the Northwest

For copies of this publication, contact:
Nature of the Northwest Information Center
800 NE Oregon Street, #28, Suite 965
Portland, Oregon, 97232
telephone (971) 673-2331
http://www.NatureNW.org

State of Oregon
Oregon Department of Geology and Mineral Industries
Vicki S. McConnell, State Geologist

OPEN-FILE REPORT O-13-23

SILICIC VOLCANISM IN THE MENAGERIE WILDERNESS AND ADJACENT REGIONS OF THE WESTERN CASCADES IN OREGON

by Geoffrey W. Cook[1], Craig M. White, and James L. Crowley
Department of Geosciences, Boise State University, Boise, Idaho

2013

[1]Present address: Scripps Institution of Oceanography, University of California, San Diego, La Jolla, CA 92093; email: gwcook@ucsd.edu

DISCLAIMER

This product is for informational purposes and may not have been prepared for or be suitable for legal, engineering, or surveying purposes. Users of this information should review or consult the primary data and information sources to ascertain the usability of the information. This publication cannot substitute for site-specific investigations by qualified practitioners. Site-specific data may give results that differ from the results shown in the publication. See the accompanying text for more details on the limitations of the methods and data used to prepare this publication.

Oregon Department of Geology and Mineral Industries Open-File Report O-13-23
Published in conformance with ORS 516.030

For copies of this publication or other information about Oregon's geology and natural resources, contact:

Nature of the Northwest Information Center
800 NE Oregon Street #28, Suite 965
Portland, Oregon 97232
(971) 673-2331
http://www.naturenw.org

For additional information:
Administrative Offices
800 NE Oregon Street #28, Suite 965
Portland, OR 97232
Telephone (971) 673-1555
Fax (971) 673-1562
http://www.oregongeology.org
http://egov.oregon.gov/DOGAMI/

TABLE OF CONTENTS

LIST OF FIGURES

LIST OF TABLES

ABSTRACT

Geologic studies within and adjacent to the Menagerie Wilderness in the Western Cascade Range indicate this region was the site of several large silicic dome-building events in middle Miocene time. Rhyolites in this area occur as flow-banded, devitrified lava flows with well-developed basal vitrophyres, coarse block-and-ash breccias, and partially eroded endogeneous domes. Three petrographically distinctive units were recognized within the dome complex: a coarsely porphyritic hornblende rhyolite (rhyolite of Rooster Rock), a less crystal rich quartz-bearing rhyolite (rhyolite of Soda Fork and a related block and ash unit), and a biotite-bearing rhyolite with abundant large phenocrysts of quartz (rhyolite of Moose Mountain). The domes and lava flows overlie an older sequence of silicic ignimbrites and are themselves overlain by younger mafic lava flows. In addition to the field and petrographic descriptions, we report 10 bulk-rock chemical analyses of lavas and dome rocks and two new radiometric dates. All the chemically analyzed rhyolites display the relatively high contents of Al_2O_3, CaO, and Sr and low abundances of Nb typical of silicic rocks in volcanic arc settings. The analyses also plot within the compositional ranges for silicic rocks in the Three Sisters and Broken Top systems of the High Cascades. The dated specimens include a rhyolite lava flow from the Soda Fork unit and an ignimbrite exposed at low elevation along U.S. Highway 20. The lava flow yielded an ^{40}Ar-^{39}Ar plateau date on plagioclase of 13.15 ± 0.24 Ma, and the ignimbrite produced a high-precision CA-TIMS U-Pb zircon date of 16.27 ± 0.02 Ma. We present the following observations based on the results of this study: (a) effusive eruptions built several rhyolite domes in the area of the present-day Menagerie Wilderness during middle Miocene time; (b) prominent rock spires within the wilderness area are probably the erosional remnants of the largest of these domes; (c) the chemical similarity between the silicic magmas erupted in this part of the Western Cascades and those erupted in adjacent parts of the High Cascades suggests both suites were derived from similar source rocks and/or had similar petrogenetic histories; (d) the association of rhyolitic domes overlying an unknown thickness of silicic ignimbrites may indicate the presence of an eroded, large, previously unrecognized caldera.

INTRODUCTION

The Cascade Range in Oregon was first divided into two distinct structural units by Callaghan (1933), who recognized an older, deformed Western Cascade sequence and a younger, relatively undeformed High Cascade sequence. Later workers subdivided the Western Cascade sequence in various ways, but most maps and reports published in the last 50 years recognized an Oligocene through early Miocene age series composed of mafic to silicic lava flows, silicic pyroclastics and volcanic sedimentary rocks, and a middle to late Miocene age series composed primarily of andesitic lavas and breccias (Peck and others, 1964; White and McBirney, 1978; Priest and others, 1983; Walker and Duncan, 1989). As more K-Ar and ^{40}Ar-^{39}Ar dates became available, Priest (1990) put the age of the older series at between 35 and 18 Ma (early Western Cascade episode) and the age of the younger series at between 17 and 7 Ma (late Western Cascade episode) and assigned rocks younger than 7 Ma to the High Cascade episode. Sherrod and Smith (2000) divided the Western Cascade volcanic sequence in Oregon into five age groups for mapping purposes: an older 45–36 Ma group, exposed only in the region south of Eugene, and four younger groups of 35–26 Ma, 25–18 Ma, 17–8 Ma, and 7–2 Ma.

More recently, du Bray and John (2011) examined the time-space-composition relations for the ancestral Cascades arc in northern California, Oregon, and Washington from a synthesis of about 3,500 bulk-rock chemical analyses and the associated age data. They subdivided the data set according to the age groupings of Sherrod and Smith (2000) but limited the youngest group to the interval between 7 and 4 Ma, following the suggestion by Hildreth (2007) that 4 Ma is the most reasonable date to mark the beginning of High Cascade magmatism. Their data showed that magmatism during the interval 25–18 Ma generated the greatest volumes of volcanic rocks as well as the largest proportions of silica-rich rocks.

The present report focuses on a sequence of silicic volcanic rocks that crop out within and adjacent to the Menagerie Wilderness, a popular rock-climbing area just north of the South Santiam Highway (U.S. Route 20) (Figure 1 and Appendix A). The silicic rocks in this area were assigned to the Little Butte Volcanic Series by Peck and others (1964)

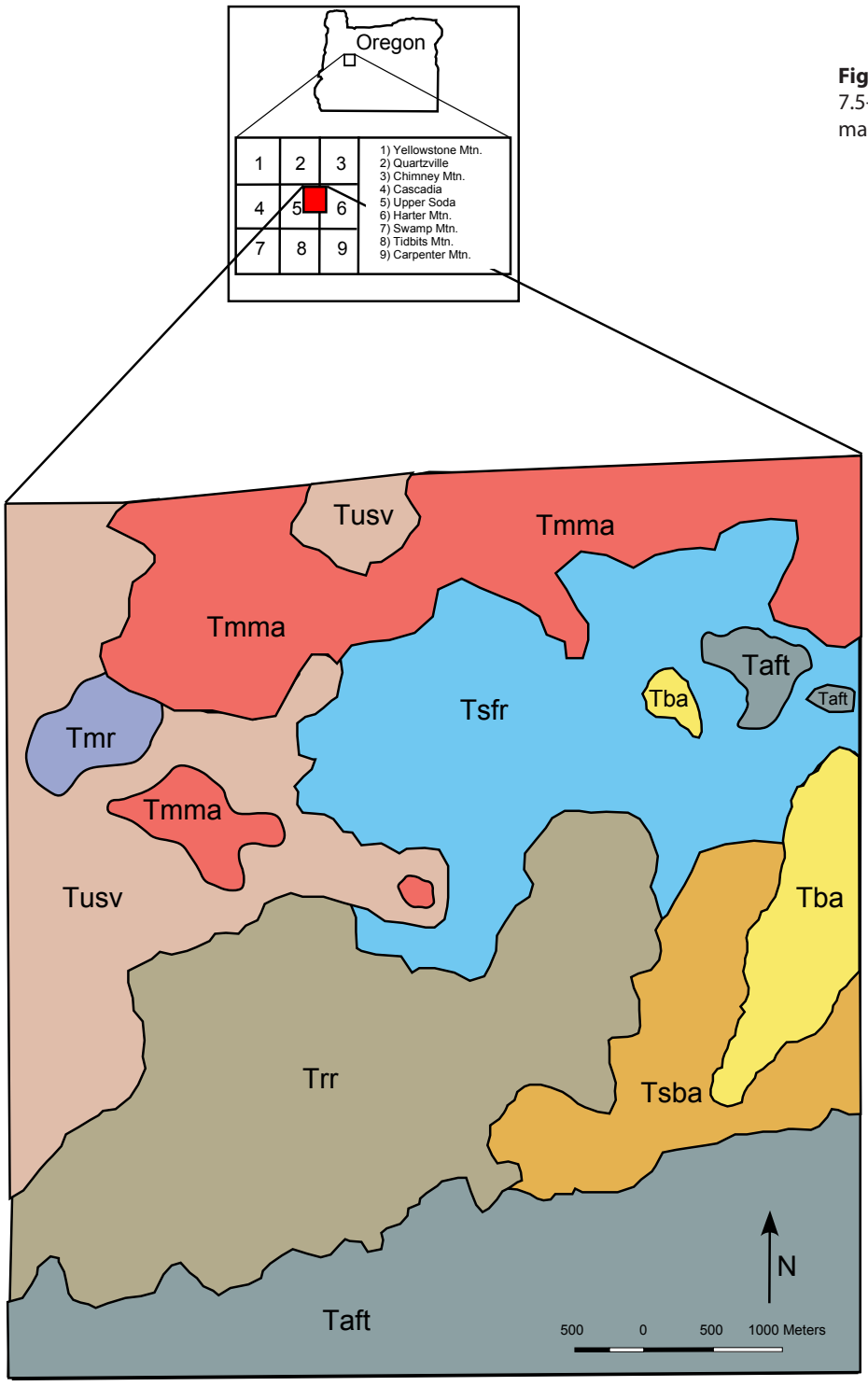

Figure 1. (top) Study area and U.S. Geological Survey 7.5-minute quadrangles. (bottom) Geologic units in map area; also see Appendix A: Map Plate.

and are shown as unit Td3 (17–25 Ma dacitic rocks) on the geologic map of Sherrod and Smith (2000). Maps of Walker and Duncan (1989) and Sherrod and Smith (2000) indicate that pyroclastic flow deposits are abundant at lower elevations on both sides of this stretch of the South Santiam River. However, most authors cited above have also noted that the silica-rich rocks in the Western Cascades are poorly characterized and poorly understood compared to the basalts and andesites. Glass shards and pumice in the pyroclastic rocks are commonly altered to clays or zeolites, making it difficult to determine the chemical compositions of the original magmas. The ages of the silicic rocks are also badly constrained because whole-rock dating is not reliable for glassy rocks and few specimens contain unaltered phenocrysts datable by argon methods. To help address the paucity of information about these rocks, we present new data on the compositions and ages of the silicic rocks in the Menagerie Wilderness and surrounding areas. These data are presented in context with the field relations in this relatively well exposed center of silicic volcanism.

STRATIGRAPHY AND DESCRIPTION OF UNITS

A geologic map of the study area was made during the summer field season of 2001; detailed descriptions of the field relations and rock units are given by Cook (2002). Eight lithologic units are distinguished on the map, six of which are silicic in composition (see Figure 1 and Appendix A). The stratigraphically lowest unit consists of a series of ignimbrites exposed along U.S. route 20 and in the valley of Soda Fork. The overlying silicic rocks are grouped into four map units based on their physical and petrographic characteristics. Most rocks in these units are flows and breccias associated with silicic dome complexes. A sixth map unit comprises a few widely separated exposures of silicic tephra and lava found mainly along logging roads in the western part of the map area. The silicic rocks are overlain by andesitic and basaltic andesite lava flows that probably belong to the latest Western Cascade and early High Cascade sequences. In this discussion, the rock name "rhyolite" is used in a broad sense for most of the silicic rocks in the map area. A discussion of the chemical compositions and classification of these rocks follows the unit descriptions.

Tba **basaltic andesite volcanics (Pliocene [?])**— Basaltic andesite lava flows, some with well-developed columnar joints. Flows are porphyritic with plagioclase phenocrysts to 2 mm and clinopyroxene phenocrysts to 2.5 mm. Unit is approximately 130 m thick.

Tmma **andesite of Moose Mountain (Pliocene [?])**— Two-pyroxene andesite and basaltic andesite lava flows. Flows are generally porphyritic with plagioclase phenocrysts visible to 5 mm and pyroxene to 2.5 mm. The unit is informally referred to as the andesite of Moose Mountain.

Tmr **rhyolite of Moose Mountain (Miocene)**— The youngest rhyolitic unit is found in the northwest region of the study area and is the smallest in area (see Figure 1 and Appendix A). Field investigations revealed a series of light-colored, porphyritic rhyolite flows approximately 130 m thick. In hand specimen, quartz (to 1 cm) and biotite (< 0.5 cm) phenocrysts are visible. A number of vent complexes were observed throughout the unit as evidenced by vertical flow banding and heightened degrees of hydrothermal alteration. Strong flow banding is pervasive throughout the unit, although the banding is not as well developed as in the Soda Fork dome complex.

In thin section these rocks have a vitric groundmass. The main phenocryst present is quartz to approximately 4 mm with numerous glass inclusions and embayments. Many of the quartz grains are partially resorbed. Feldspars are the next most plentiful phenocrysts, with plagioclase (An_{52}) present as blocky and clean crystals to 3 mm; these exhibit both albite twinning and oscillatory zoning. Anorthoclase is also present as blocky, euhedral crystals to 2 mm. Biotite is the main ferromagnesian phase, occurring as platy, euhedral crystals to 0.8 mm; many of these are altered to opaque minerals. Glomerocrysts of quartz, feldspars, and biotite to approximately 3 mm are common.

Tusv **undifferentiated silicic volcanics (Miocene)**— This unit is found predominantly in the northeast portion of the study area (Figure 1). The unit is poorly exposed (it is composed of ashy, easily eroded rocks) and covered by dense vegetation. Although mapped as a single unit, it may represent a variety of rocks of different ages and stratigraphic positions. Consequently, a great deal of uncertainty about the true nature of this unit exists. The few exposed sections consist of a series of highly altered, silicic volcanic deposits including ignimbrites and flow-banded

rhyolite. The deposit is estimated to be at least 330 m thick. Because of alteration in these rocks, good samples for petrography or geochemistry could not be obtained.

Tsba **block and ash flows of Soda Fork (Miocene)**— A coarse breccia unit is situated in the valley of Soda Fork and conformably overlies the distal end of the Soda Fork flow-banded rhyolite (Figure 1 and Appendix A). The rocks are well exposed in several large road cuts along U.S. Forest Service road FR-2041. The unit is a buff-colored, matrix-supported volcanic breccia approximately 240 m hick. Angular rhyolite blocks up to 30 cm across display flow banding similar to that seen in rhyolite of the Soda Fork formation (Tsfr). No evidence of prismatic jointing or welding of the juvenile material was found during the field investigation, suggesting that the material was relatively cool when deposited.

The matrix of these rocks is composed of fine ash. Pumice lapilli to 4-5 mm are present throughout the matrix. In thin section, crystals of altered feldspars to 4 mm (most are corroded), quartz to 1 mm, and opaque grains are abundant. The rocks are hydrothermally altered, with reddish oxidation and many calcite veins.

Tsfr **rhyolite of Soda Fork (Miocene)**— This unit conformably overlies the rhyolite of Rooster Rock (Trr) and is composed of several nested rhyolitic domes approximately 430 m in total thickness. Although most of the unit is devitrified, numerous individual flows were observed with prominent basal vitrophyres. Several vent areas were identified by the presence of vertical, flow-banded lavas and high degrees of hydrothermal alteration (abundant lithophysae). Flow banding is dominant throughout the unit (Figure 2). In hand specimen, these rocks are light-colored, porphyritic rhyolites with plagioclase phenocrysts to 0.5 cm.

In thin section the flow banding evident in hand specimen is present as mono-mineralogic bands of secondary quartz and opaque minerals. Phenocrysts comprise 20% of the modal percentage of the rock. Minerals present include plagioclase (An^{45}) and anorthoclase grains to 4 mm, with most highly altered and containing glass inclusions; quartz phenocrysts to 2 mm with some glass inclusions were also observed. Glomeroporphyritic masses of quartz, plagioclase, and alkali feldspar are present to approximately 5 mm.

Trr **rhyolite of Rooster Rock (Oligocene [?])**— The rhyolites of Rooster Rock are light-colored, porphyritic rocks with abundant phenocrysts of hornblende and plagioclase. Field observations and cross sections suggest the unit is a dome complex (endogenous) at least 800 m thick. The unit is noteworthy for its abundance of tall, delicate spires, some of which are 150 m high (Figure 3). In thin section the rocks are characterized by a highly altered, devitrified groundmass containing small quartz grains. Plagioclase phenocrysts to 5 mm are abundant and have a distinctive blocky appearance, exhibit oscillatory zoning and commonly have both glass inclusions and poikilitically enclosed opaques (Ti-magnetite). Many of the plagioclase phenocrysts have been partially resorbed, suggesting disequilibrium reactions. Some alkali feldspar (anorthoclase) is present. Quartz phenocrysts to approximately 4 mm are abundant; many of these contain embayments, suggesting that these grains have also been partially resorbed. In addition, much of the quartz contains small glass inclusions. The dominant ferromagnesian phenocryst is hornblende, which occurs as large (4-5 mm) grains. Most of the hornblende is corroded, and many grains are composed mainly of opaque oxides. Small opaques (to 0.5 mm) are also found as phenocrysts. Large (up to 5-6 mm) glomeroporphyritic masses are composed of plagioclase, quartz, hornblende, and oxides.

Taft **ash flow tuffs of Route 20 (Oligocene [?])**— These tuffs are exposed in the valley of the South Santiam River along U.S. Route 20; collectively, they comprise a thickness of at least 570 m. The unit consists of at least eight nonwelded to moderately welded, grayish to buff colored ignimbrites. Individual flow units range in thickness from 20 to 50 m. The ignimbrites contain mafic to intermediate lithic fragments up to 2 cm in size and pumice lapilli from 1 to 2 cm. Fall deposits up to 2 m thick are interbedded with ignimbrites throughout the unit. Debris flows of considerable thickness (up to 45 m) occur in isolated exposures. Crystals present in thin sections are considerably altered and include plagioclase, quartz, pyroxenes, and hornblende. Calcite veins are abundant and reflect evidence of hydrothermal alteration.

Figure 2. Photograph of flow-banded rhyolite of Soda Fork (unit Tsfr). Location approximately 44.429888, –122.259466 (+44° 25' 47.60", –122° 15' 34.08").

Figure 3. Photographs of rhyolite spires of Rooster Rock (unit Trr). Location of spires approximately 44.428386, –122.281444 (+44° 25' 42.19", –122° 16' 53.20").

GEOCHEMISTRY

Chemical analyses of 10 specimens collected from the three main dome and flow units within the mapped area are presented in Table 1. The locations of the analyzed rocks are shown on the geologic map (Appendix A). The rocks were analyzed for major oxides and trace elements using the X-ray fluorescence instrument at the Washington State University (WSU) GeoAnalytical Lab. One specimen from each unit was also analyzed for additional trace elements using the WSU laboratory's inductively coupled plasma mass spectrometer (ICP-MS) facility. As noted above, chemical analyses of silica-rich volcanics in the Western Cascades cannot always be inferred to represent magma compositions owing to the common occurrence of post-depositional alteration and the presence of lithic fragments in pyroclastic rocks. To minimize this problem, all analyzed specimens are from lava flows or domes and thin sections were examined to screen out rocks showing clear evidence of hydrothermal alteration. A few analyses were discarded because they showed geochemical evidence for post-crystallization alteration according to the criteria suggested by du Bray and John (2011). Nonetheless, nearly all of the analyzed silicic rocks experienced some degree of high-temperature devitrification and vapor phase crystallization that could have slightly modified their bulk compositions. With that caveat, the chemical compositions of all of the analyzed rocks are rhyolites based on the TAS diagram of LeBas and others (1986), and all are slightly to moderately peraluminous based on their Shand index (Maniar and Piccoli, 1989).

The major oxide compositions of rocks in each of the three different lava and dome units can be compared by referring to the plots in Figure 4. The compositional ranges of about 80 dacites and rhyolites from the Three Sisters and Broken Top volcanic systems (Hill, 1992) are also shown in this figure to provide a comparison with the Quaternary silicic rocks erupted in the nearby High Cascades. The samples from units Trr (rhyolite of Rooster Rock) and Tsfr (rhyolite of Soda Fork) show considerable scatter on the Harker diagrams and do not plot in distinctively separate fields. The two analyzed specimens from unit Tmr (rhyolite of Moose Mountain) plot away from the others owing mainly to their greater SiO_2 contents, but also because of their relatively lower K_2O and greater CaO abundances. All the Menagerie area rhyolites plot within or close to the trends for High Cascade rhyolites from the Three Sisters and Broken Top systems. The chondrite-normalized rare-earth-element (REE) concentrations in one sample from

Table 1. Major and trace element chemical data.

Unit	Sample	SiO_2	TiO_2	Al_2O_3	FeO	MnO	MgO	CaO	K_2O	P_2O_5	Na_2O	Ni	Sc	V	Ba	Rb	Sr	Zr	Y	Nb	Cu	Zn	Pb
Tsfr	WC77	73.82	0.294	14.45	1.6	0.029	0.17	0.7	3.57	0.073	5.28	9	7	22	782	100	177	180	22	13.4	3	51	7
Tsfr	WC80	76.58	0.31	12.78	1.73	0.011	0.11	0.54	4.27	0.062	2.97	4	6	14	703	131	120	212	32	13.7	1	15	10
Tsfr	WC24	71.39	0.253	16.19	1.58	0.064	0.18	0.49	2.51	0.047	6.97	6	6	7	526	97	97	297	31	16.1	3	68	8
Tsfr	WC30	74.22	0.339	14.1	2.12	0.01	0.12	1.36	2.86	0.067	4.41	5	6	19	665	75	150	238	18	13.5	2	41	16
Tsfr	WC41	74.67	0.338	13.5	2.03	0.019	0.12	1.1	3.92	0.057	3.71	5	6	20	649	85	131	221	20	11.9	7	23	13
Tmr	WC79	77.87	0.209	12.38	1.09	0.009	0.23	1.26	2.83	0.028	3.53	5	10	8	662	79	131	140	15	10.9	0	20	8
Trr	WC54	73.19	0.357	14.46	2.39	0.033	0.56	0.51	3.89	0.088	3.23	6	8	25	693	146	138	236	19	12.5	0	47	9
Trr	WC32	71.8	0.386	14.14	2.53	0.033	0.74	1.6	2.79	0.109	4.05	3	8	23	691	77	296	213	18	11.5	0	50	11
Trr	WC33	72.71	0.377	14.64	2.42	0.033	0.52	0.48	3.94	0.087	3.17	3	4	18	686	149	137	246	22	13.2	0	56	10
Trr	WC64	74.74	0.239	14.08	1.55	0.032	0.17	0.45	3.26	0.035	4.64	3	7	24	813	93	124	142	15	11.4	0	27	8

Unit	Sample	La	Ce	Pr	Nd	Sm	Eu	Tb	Dy	Ho	Er	Tm	Yb	Ba	Th	Nb	Y	Hf	Ta	Pb	Rb	Cs	Sr	Sc	Zr	U	Lu	Gd
Tsfr	WC-41	23.93	44.92	4.93	18.87	4.11	0.9	0.6	3.72	0.75	2.14	0.35	2.29	662	7.95	10.98	20.16	6.07	0.92	12.82	84	2.06	133	5.3	225	2.47	0.37	3.65
Tmr	WC-78	22.92	38.84	3.99	14.02	2.76	0.58	0.42	2.56	0.52	1.51	0.24	1.55	661	8.71	8.5	15.83	3.77	0.86	10.66	75.5	2.55	129	3.4	131	1.77	0.26	2.49
Trr	WC-54	24.27	44.56	4.7	17.55	3.7	0.74	0.53	3.25	0.66	1.91	0.32	2.06	687	9.08	11.46	19.39	6.27	0.97	10.71	144.8	19.58	138	6.8	243	2.6	0.34	3.19

each of the three units are plotted in Figure 5, along with the range of REE abundances in the silicic rocks from the Three Sisters-Broken Top systems (Hill, 1992). The chondrite-normalized REE trends are similar for all three of the Menagerie rhyolites, with the high-SiO_2 specimen from unit Tmr having the lowest REE abundances. Once again, the Menagerie rhyolites do not differ substantially in composition from the High Cascade rocks.

A discussion of the petrogenesis of the Menagerie rhyolites is beyond the scope of this report and is not warranted

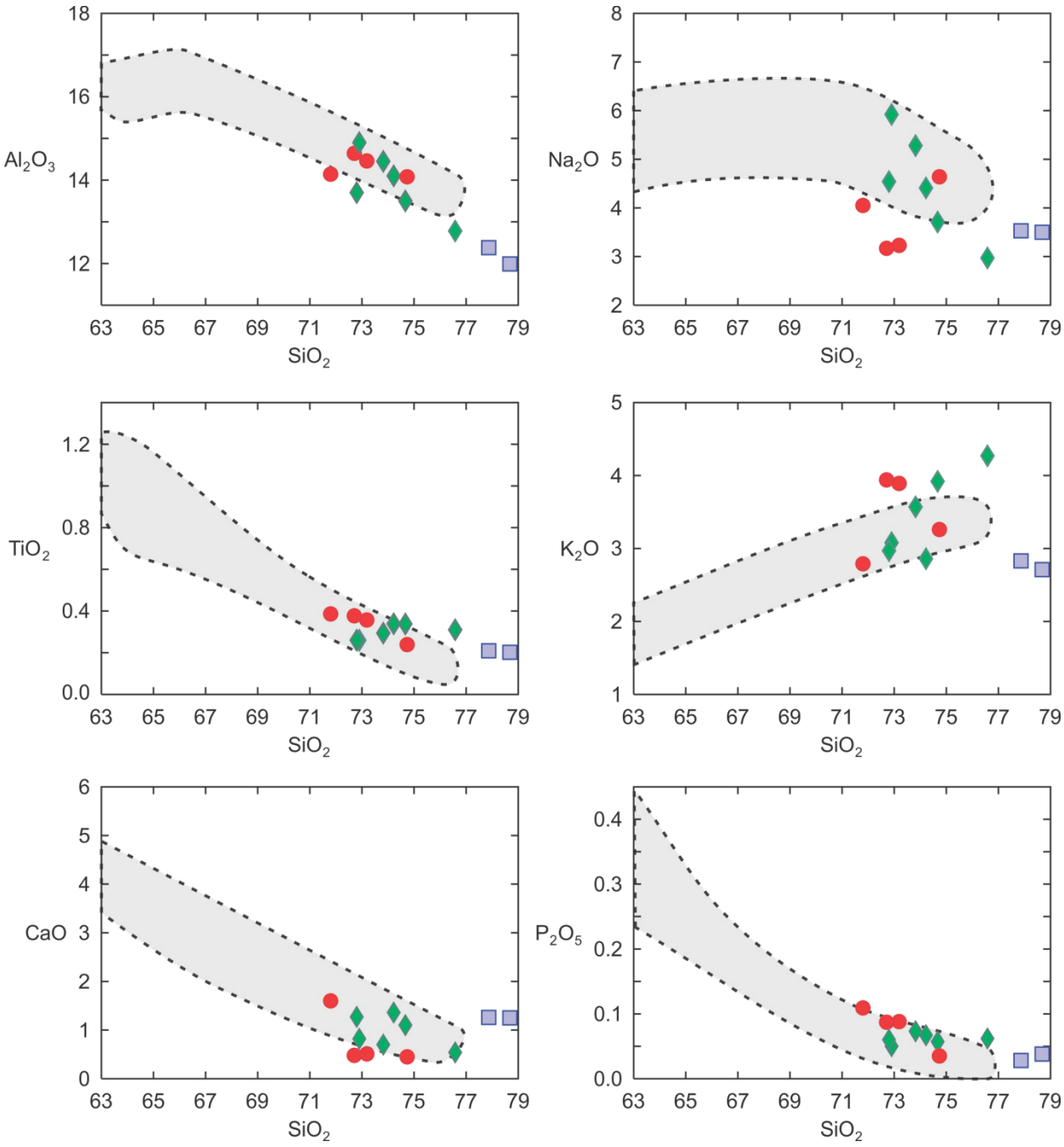

Figure 4. Major oxide geochemical plots for rhyolites from the Menagerie Wilderness and surrounding areas. Specimens from map unit Trr are indicated by circles, diamonds are unit Tsfr, and squares are unit Tmr. The shaded area indicates the range of analyses of dacites and rhyolites from the Three Sisters and Broken Top areas from Hill (1992).

by the limited data set; however, we make a few observations below based on the geochemical analyses. Not surprisingly, the Menagerie rhyolites display the relatively high contents of Al_2O_3, CaO, and Sr and low abundances of Nb that typically distinguish rhyolites in volcanic arcs from rhyolites in other continental tectonic settings (see e.g., Ayalew and Ishiwatari, 2011). The roughly L-shaped REE patterns and modest negative Eu anomalies shown by these rocks in Figure 5 are also a characteristic of silicic magmas produced in the "wet" magmatic environments associated with subduction (e.g., Bachmann and Bergantz, 2008). Perhaps more surprising is the close geochemical similarity between the Menagerie rhyolites and rhyolites in the High Cascades. Although the Menagerie rhyolites erupted about 40 km west of the present High Cascades and at a substantially earlier stage in the evolution of the Cascade arc, we do not see any systematic chemical differences between the two suites. This observation contrasts with the spatial and temporal chemical variations noted for some other arcs (e.g., Gill [1981]) and may imply that the crust is relatively uniform in composition and thickness throughout this region. Unit Tmr is an exception inasmuch as its SiO_2 content is greater than that of any of the other Menagerie rhyolites as well as any of the High Cascade rhyolites analyzed by Hill (1992). The high SiO_2 content and relatively low abundances of alkalis and excluded trace elements in these rocks suggest the magmas that formed them may have had a different source and/or evolutionary history than the other silicic magmas in this region. The age of the unit has not been determined, but field relations indicate it is the youngest rhyolite in the map area.

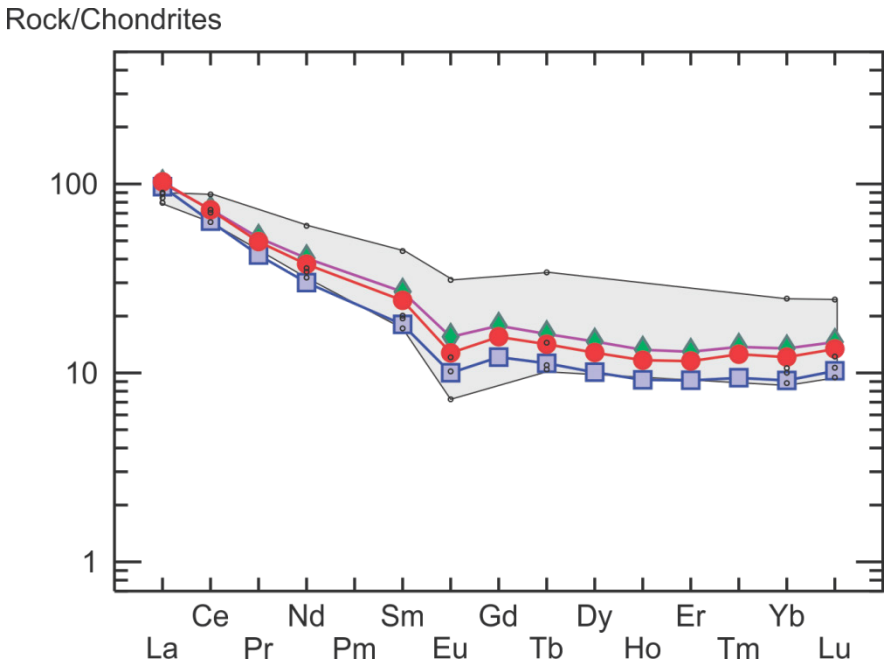

Figure 5. Chondrite normalized REE diagram for rhyolites from the Menagerie Wilderness and surrounding areas. Symbols are the same as for Figure 5. The shaded area indicates the range of analyses of dacites and rhyolites from the Three Sisters and Broken Top areas from Hill (1992).

RADIOMETRIC DATES

Radiometric dates were obtained for specimens from two of the rhyolite units exposed in the Menagerie area. A lava flow in unit Tsfr yielded an ^{40}Ar-^{39}Ar date of 13.15 ± 0.24 Ma on plagioclase, and an ignimbrite in unit Taft exposed along U.S. Highway 20 yielded a high-precision CA-TIMS U-Pb zircon date of 16.27 ± 0.02 Ma.

The specimen dated by the ^{40}Ar-^{39}Ar method was collected from the basal vitrophyre of a flow-banded rhyolitic lava flow exposed at an elevation of about 795 m (2,600 feet) in the upper Soda Fork drainage (UTM-NAD83 is 558808 E, 4922215 N). Dating of this specimen was performed in 2005 at the Noble Gas Mass Spectrometry Laboratory at the College of Oceanic and Atmospheric Sciences at Oregon State University. We cite the weighted plateau date obtained from six incremental heating steps using a bulk plagioclase separate (Figure 6).

The specimen dated by the chemical abrasion thermal ionization mass spectrometry (CA-TIMS) U-Pb method was collected from the middle of an ignimbrite exposed along the north side of U.S. Highway 20 across from the U.S. Forest Service Fern View Campground (UTM-NAD83 is 555448E, 4917146N). Dating of this specimen was performed in 2012 in the Boise State University Isotope Geology Laboratory. A description of the procedures used for high-precision U-Pb dating in this laboratory is given in Appendix B and can also be found at http://earth.boisestate.edu/isotope/.

Seven grains were analyzed by CA-TIMS, and one of the grains was broken into two fragments that were dated separately. The seven youngest dates are equivalent and yield a weighted mean $^{206}Pb/^{238}U$ date of 16.27 ± 0.02 Ma (MSWD = 0.3) (Figure 7). This is the interpreted igneous crystallization age. Errors with addition of the tracer calibration and decay constant uncertainties are ± 0.02 and ± 0.03 Ma, respectively. One other date is 16.43 ± 0.07 Ma. The seven zircon crystals dated by CA-TIMS were selected from 73 crystals that were analyzed earlier for trace element concentrations by laser ablation inductively coupled plasma mass spectrometry (LA-ICPMS) at Boise State University. A description of these procedures is given in Appendix C. Zircon crystallization temperatures were estimated for these crystals using the Ti-in-zircon thermometer of Ferry and Watson (2007). The mean temperature of these estimates is 770°C.

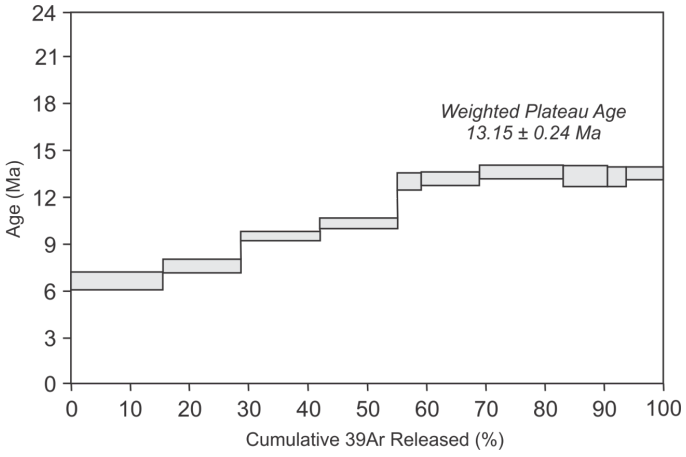

Figure 6. ^{40}Ar-^{39}Ar incremental heating plateau diagram for a bulk plagioclase separate from a rhyolite lava flow (specimen SS04-22) in unit Tsfr.

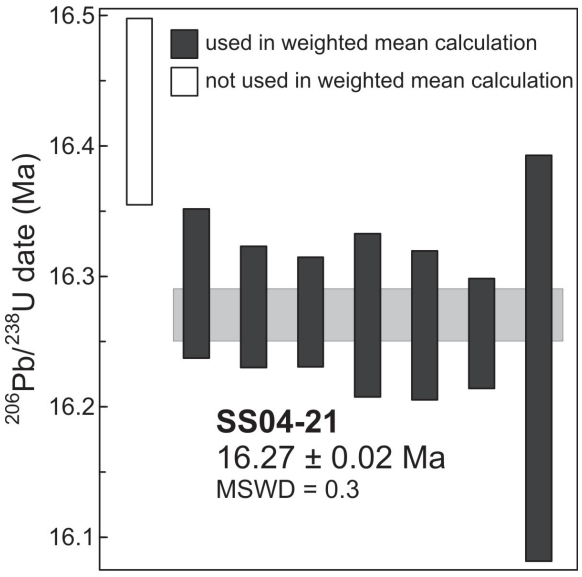

Figure 7. Plot of $^{206}Pb/^{238}U$ dates for zircons extracted from an ignimbrite (specimen SS04-21) in unit Taft exposed along U.S. Highway 20. Plotted with Isoplot 3.0 (Ludwig, 2003). Error bars are at the 95% confidence interval. Weighted mean date is represented by the grey box behind the error bars.

CONCLUSIONS

Volcanic rocks within and adjacent to the Menagerie Wilderness are mainly composed of rhyolitic flows and breccias that appear to be related to a complex of overlapping volcanic domes. The largest of these domes is composed of coarsely porphyritic hornblende rhyolite that forms Rooster Rock and the other prominent spires within the wilderness area. The entire dome complex is probably younger than the 16.27 ± 0.02 Ma ignimbrite exposed along U.S. Highway 20, and it is likely that most of the complex had formed by the time the Soda Fork flows erupted around 13.15 ± 0.24 Ma. Although it is difficult to know the precise geologic setting for these eruptions, the relatively large size of the dome complex and the lack of mafic rocks within or beneath the silicic lavas suggest they are not minor components of a larger andesitic system. Because the Menagerie area domes appear to overlie only slightly older ignimbrites, the domes could have been erupted at the end of a much larger episode of explosive rhyolitic volcanism that took place in this part of the Western Cascades in middle Miocene time.

REFERENCES

Ayalew, D., and Ishiwatari, A., 2011, Comparison of rhyolites from continental rift, continental arc and oceanic island arc: implication for the mechanism of silicic magma generation: Island Arc, v. 20, p. 78–93.

Bachmann, O., and Bergantz, G. W., 2008, Rhyolites and their source mushes across tectonic settings: Journal of Petrology, v. 49, no. 12, p. 2277–2285.

Callaghan, E., 1933, Some features of the volcanic sequence in the Cascade Range in Oregon: Eos, Transactions of the American Geophysical Union, v. 6, p. 243–249.

Cook, G. W., 2002, Geology and geochemistry of volcanic rocks of the Menagerie Wilderness, Western Cascades, Oregon: Boise, Idaho, Boise State University, M.S. thesis, 77 p.

du Bray, E. A. and John, D. A., 2011, Petrologic, tectonic, and metallogenic evolution of the Ancestral Cascades magmatic arc, Washington, Oregon, and northern California: Geosphere, v. 7, p. 1102–1133.

Ferry, J. M., and Watson, E. B., 2007, New thermodynamic models and revised calibrations for the Ti-in-zircon and Zr-in-rutile thermometers: Contributions to Mineralogy and Petrology, v. 154, p. 429–437.

Gill, J. B., 1981, Orogenic andesites and plate tectonics: Berlin, Springer Publishing, 231 p.

Hildreth, W., 2007, Quaternary magmatism in the Cascades: geologic perspectives: U.S. Geological Survey Professional Paper 1744, 125 p.

Hill, B. E., 1992, Petrogenesis of compositionally distinct silicic volcanoes in the Three Sisters region of the Oregon Cascade Range: the effects of crustal extension on the development of continental arc silicic magmatism: Oregon State University, Ph.D. dissertation, 235 p.

Ludwig, K. R., 2003, User's manual for Isoplot 3.00: Berkeley, Calif., Berkeley Geochronology Center, 70 p.

Maniar, P. D., and Piccoli, P. M., 1989, Tectonic discrimination of granitoids: Geological Society of America Bulletin 101, p. 635–643.

Peck, D. L., Griggs, A. B., and Schlicker, H. G., Wells, F. G., and Dole, H. M., 1964, Geology of the central and northern parts of the western Cascade Range in Oregon: U. S. Geological Survey Professional Paper 449, 56 p.

Priest, G. R., 1990, Volcanic and tectonic evolution of the Cascade volcanic arc, central Oregon: Journal of Geophysical Research, v. 95, p. 19,683–19,599.

Priest, G. R., Woller, N. M., and Black, G. L., and Evans, S. H., 1983, Overview of the geology of the central Oregon Cascade Range, *in* Priest, G. R., and Vogt, B. F., eds., Geology and geothermal resources of the central Oregon Cascade Range: Oregon Department of Geology and Mineral Industries Special Paper 15, p. 3–28.

Sherrod, D. R., and Smith, J. G., 2000, Geologic map of upper Eocene to Holocene volcanic and related rocks of the Cascade Range, Oregon: U.S. Geological Survey Geological Investigations Series Map I-2569, scale 1:500,000.

Walker, G. W., and Duncan, R. A., 1989, Geologic map of the Salem 1 degrees by 2 degrees quadrangle, western Oregon: U.S. Geological Survey Miscellaneous Investigations Series Map I-1893, scale 1:250,000.

White, C. M., and McBirney, A. R., 1978, Some quantitative aspects of orogenic volcanism in the Oregon Cascades, *in* Smith, R. B., and Eaton, G. P., eds., Cenozoic tectonics and regional geophysics of the Western Cordillera: Geological Society of America Memoir 152, p. 369–398.

APPENDIX A: MAP PLATE (SEPARATE PDF)

Geologic Map of Part of the Upper Soda and Harter Mountain 7.5-Minute Quadrangles, Oregon, scale 1:12,000

APPENDIX B: CA-TIMS METHODS

U-Pb dates were obtained by the chemical abrasion isotope dilution thermal ionization mass spectrometry (CA-TIMS) method from analyses composed of single zircon grains or fragments of grains (Table 1 in main text). Zircon grains were separated from rocks using standard techniques and mounted in epoxy and polished until the centers of the grains were exposed. Cathodoluminescence (CL) images were obtained with a JEOL JSM-1300 scanning electron microscope and Gatan MiniCL. Zircon was analyzed by laser ablation inductively coupled plasma mass spectrometry (LA-ICPMS) before being removed from the epoxy mounts and subjected to a modified version of the chemical abrasion method of Mattinson (2005). Grains were selected for dating based on the chemistry obtained by LA-ICPMS.

Zircon was placed in a muffle furnace at 900°C for 60 hours in quartz beakers. Single grains were then transferred to 3 ml Teflon PFA beakers and loaded into 300 µl Teflon PFA microcapsules. Fifteen microcapsules were placed in a large-capacity Parr vessel, and the crystals partially dissolved in 120 µl of 29 M HF for 12 hours at 180°C. The contents of each microcapsule were returned to 3 ml Teflon PFA beakers, the HF removed and the residual grains immersed in 3.5 M HNO_3, ultrasonically cleaned for an hour, and fluxed on a hotplate at 80°C for an hour. The HNO_3 was removed and the grains were rinsed twice in ultrapure H_2O before being reloaded into the same 300 µl Teflon PFA microcapsules (rinsed and fluxed in 6 M HCl during sonication and washing of the grains) and spiked with the Boise State University mixed ^{233}U-^{235}U-^{205}Pb tracer solution. These chemically abraded grains were dissolved in Parr vessels in 120 µl of 29 M HF with a trace of 3.5 M HNO_3 at 220°C for 48 hours, dried to fluorides, and then redissolved in 6 M HCl at 180°C overnight. U and Pb were separated from the zircon matrix using an HCl-based anion-exchange chromatographic procedure (Krogh, 1973), eluted together and dried with 2 µl of 0.05 N H_3PO_4.

Pb and U were loaded on a single outgassed Re filament in 5 µl of a silica-gel/phosphoric acid mixture (Gerstenberger and Haase, 1997), and U and Pb isotopic measurements were made on a GV Isoprobe-T multicollector thermal ionization mass spectrometer equipped with an ion-counting Daly detector. Pb isotopes were measured by peak-jumping all isotopes on the Daly detector for 100 to 160 cycles, and corrected for 0.18 ± 0.06%/a.m.u. (2σ error) mass fractionation. Transitory isobaric interferences due to high-molecular weight organics, particularly on ^{204}Pb and ^{207}Pb, disappeared within approximately 30 cycles, while ionization efficiency averaged 104 cps/pg of each Pb isotope. Linearity (to ≥1.4 × 106 cps) and the associated dead time correction of the Daly detector were monitored by repeated analyses of NBS982, and have been constant since installation. Uranium was analyzed as UO^{2+} ions in static Faraday mode on 1011-ohm resistors for 200 to 250 cycles, and corrected for isobaric interference of $^{233}U^{18}O^{16}O$ on $^{235}U^{16}O^{16}O$ with an $^{18}O/^{16}O$ of 0.00206. Ionization efficiency averaged 20 mV/ng of each U isotope. U mass fractionation was corrected using the known $^{233}U/^{235}U$ ratio of the ET535 tracer solution.

Two to six analyses were performed for each of 10 samples. Weighted mean $^{206}Pb/^{238}U$ dates were calculated from equivalent dates using Isoplot 3.0 (Ludwig, 2003) and are interpreted as being the igneous crystallization ages for the plutonic rocks. Errors on the weighted mean $^{206}Pb/^{238}U$ dates are the internal errors based on analytical uncertainties only, including counting statistics, subtraction of tracer solution, and blank and initial common Pb subtraction. They are given at the 2σ confidence interval. These errors should be considered when comparing our dates with $^{206}Pb/^{238}U$ dates from other laboratories that used the same Boise State University tracer solution or a tracer solution that was cross-calibrated using EARTHTIME gravimetric standards. When comparing our dates with those derived from other geochronological methods using the U-Pb decay scheme (e.g., laser ablation ICPMS), a systematic uncertainty in the tracer calibration should be added to the internal error in quadrature. When comparing our dates with those derived from other decay schemes (e.g., $^{40}Ar/^{39}Ar$, ^{187}Re-^{187}Os), systematic uncertainties in the tracer calibration and ^{238}U decay constant (Jaffey and others, 1971) should be added to the internal error in quadrature. Errors on the $^{206}Pb/^{238}U$ dates from individual grains are also given at the 2σ confidence interval.

U-Pb dates and uncertainties were calculated using the algorithms of Schmitz and Schoene (2007), $^{235}U/^{205}Pb$ of

77.93 and $^{233}U/^{235}U$ of 1.007066 for the Boise State University tracer solution, and U decay constants recommended by Jaffey and others (1971). $^{206}Pb/^{238}U$ ratios and dates were corrected for initial ^{230}Th disequilibrium using a Th/U[magma] = 3.0 ± 0.3 using the algorithms of Crowley and others (2007), resulting in an increase in the $^{206}Pb/^{238}U$ dates of ~0.09 Ma. All common Pb in analyses was attributed to laboratory blank and subtracted based on the measured laboratory Pb isotopic composition and associated uncertainty. U blanks are difficult to measure precisely but are estimated at 0.07 pg.

Seven aliquots of the EARTHTIME 100 Ma synthetic solution were measured during this experiment using the Boise State University tracer solution and the same mass spectrometry methods described above. Each aliquot was 4-6 pg of radiogenic Pb, slightly smaller than the average analysis measured during the experiment. The weighted mean $^{206}Pb/^{238}U$ and $^{207}Pb/^{235}U$ dates are 100.08 ± 0.03 Ma and 100.04 ± 0.13 Ma, respectively. These dates agree with the known dates determined by analysis of large aliquots measured with the EARTHTIME mixed ^{233}U-^{235}U-^{202}Pb-^{205}Pb tracer solution (D. Condon, unpublished data, 2012).

APPENDIX C: LA-ICPMS METHODS

Zircon was analyzed by laser ablation inductively coupled plasma mass spectrometry (LA-ICPMS) using a Thermo-Electron X-Series II quadrupole ICPMS and New Wave Research UP-213 Nd:YAG UV (213 nm) laser ablation system. In-house analytical protocols, standard materials, and data reduction software were used for acquisition and calibration of a suite of high field strength elements (HFSE) and rare earth elements (REE). Zircon was ablated with a laser spot 25 µm wide using fluence and pulse rates of 5 J/cm^2 and 10 Hz, respectively, during a 30-sec analysis (15 sec gas blank, 45 sec ablation) that excavated a pit ~25 µm deep. Ablated material was carried by a 1.2 L/min He gas stream to the nebulizer flow of the plasma. Dwell times were 5 ms for Si and Zr; 100 ms for ^{49}Ti; and 10 ms all other HFSE and REE. Background count rates for each analyte were obtained prior to each spot analysis and subtracted from the raw count rate for each analyte. Temperature are calculated from the Ti-in-zircon thermometer (Ferry and Watson, 2007). Because there are no constraints on the activity of TiO_2 in the source magmas, an average value in crustal rocks of 0.6 was used.

REFERENCES FOR APPENDICES

Crowley, J. L., Schoene, B., and Bowring, S. A., 2007, U-Pb dating of zircon in the Bishop Tuff at the millennial scale: Geology, v. 35, p. 1123–1126.

Ferry, J. M., and Watson, E. B., 2007, New thermodynamic models and revised calibrations for the Ti-in-zircon and Zr-in-rutile thermometers: Contributions to Mineralogy and Petrology, v. 154, p. 429–437.

Gerstenberger, H., and Haase, G., 1997, A highly effective emitter substance for mass spectrometric Pb isotope ratio determinations: Chemical Geology, v. 136, p. 309–312.

Jaffey, A. H., Flynn, K. F., Glendenin, L. E., Bentley, W. C., and Essling, A. M., 1971, Precision measurements of half-lives and specific activities of ^{235}U and ^{238}U: Physical Review C, v. 4, p. 1889–1906.

Krogh, T. E., 1973, A low contamination method for hydrothermal decomposition of zircon and extraction of U and Pb for isotopic age determination: Geochimica et Cosmochimica Acta, v. 37, p. 485–494.

Ludwig, K. R., 2003, User's manual for Isoplot 3.00: Berkeley, Calif., Berkeley Geochronology Center, 70 p.

Mattinson, J. M., 2005, Zircon U-Pb chemical abrasion ("CA-TIMS") method: combined annealing and multi-step partial dissolution analysis for improved precision and accuracy of zircon ages: Chemical Geology, v. 220, p. 47–66.

Schmitz, M. D., and Schoene, B., 2007, Derivation of isotope ratios, errors and error correlations for U-Pb geochronology using ^{205}Pb-^{235}U-(^{233}U)-spiked isotope dilution thermal ionization mass spectrometric data: Geochemistry, Geophysics, Geosystems (G3) 8, Q08006, doi:10.1029/2006GC001492